Spectral line imaging

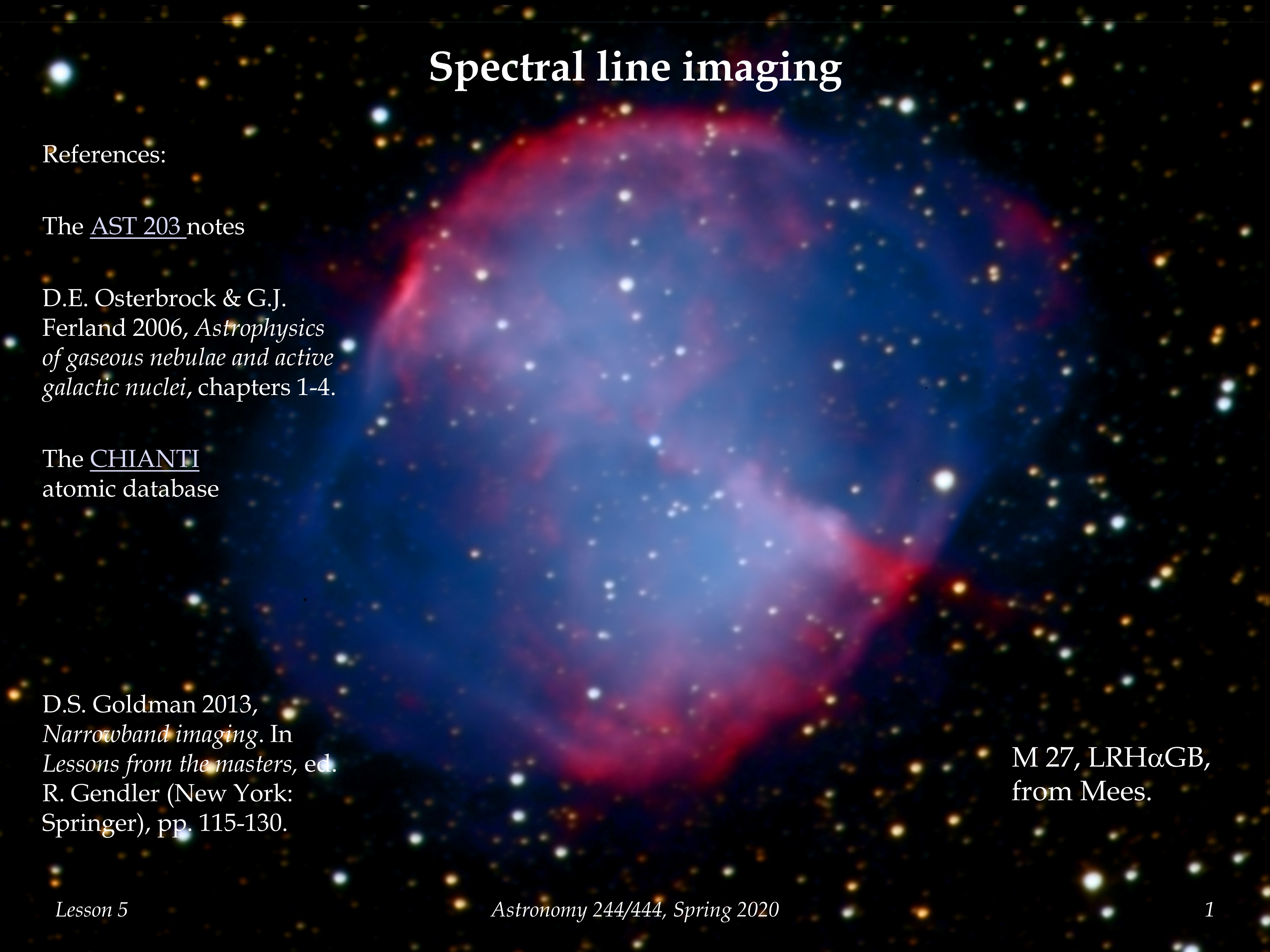

References:

The AST 203 notes

D.E. Osterbrock & G.J. Ferland 2006, *Astrophysics of gaseous nebulae and active galactic nuclei*, chapters 1-4.

The CHIANTI atomic database

D.S. Goldman 2013, *Narrowband imaging*. In *Lessons from the masters,* ed. R. Gendler (New York: Springer), pp. 115-130.

M 27, LRHαGB, from Mees.

Spectral line imaging at visible and infrared wavelengths

All spectroscopy involves the use of interference to distinguish one wavelength from another.

- The larger the phase difference between signals – or path-length difference, in most of our applications – the more finely wavelengths can be discriminated.
- **Spectral resolution** $\Delta\lambda/\lambda$ at wavelength λ is characterized by the instrument's bandwidth $\Delta\lambda$ for a truly monochromatic signal.
  - Two signals at wavelengths separated by $\geq \Delta\lambda$ are **resolved**; otherwise they're **unresolved**.

Interference filters

This semester we use multilayer dielectric interference filters, in front of the CCD, to make spectral line images.

- See the AST 203 notes to learn how these are designed and built.
- Upside: compact, extremely uniform in transmission and bandwidth.
- Downside: non-adjustable; hard to get high enough spectral resolution to isolate single lines; not the ultimate in sensitivity.
- In some wavelength ranges one has to have extra filters set for an off-line wavelength, to subtract continuum emission.

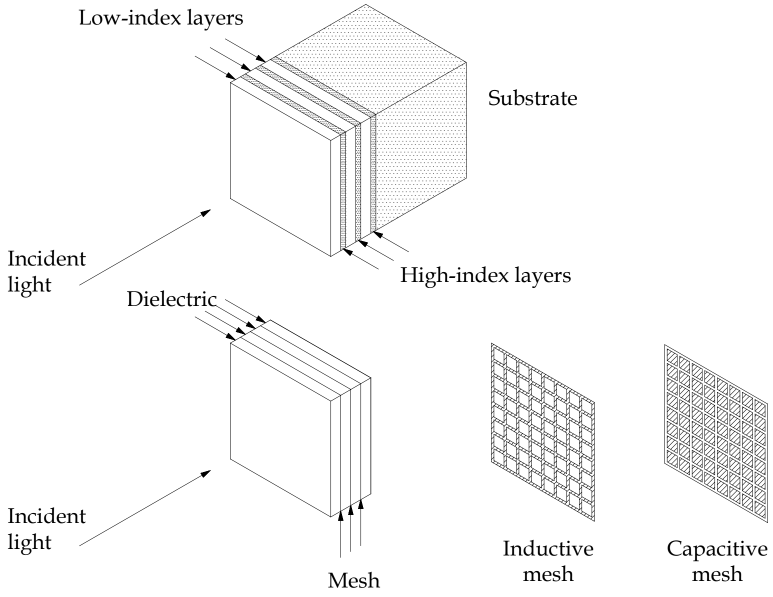

Spectrographs

More sophisticated and more wavelength-selective instruments:

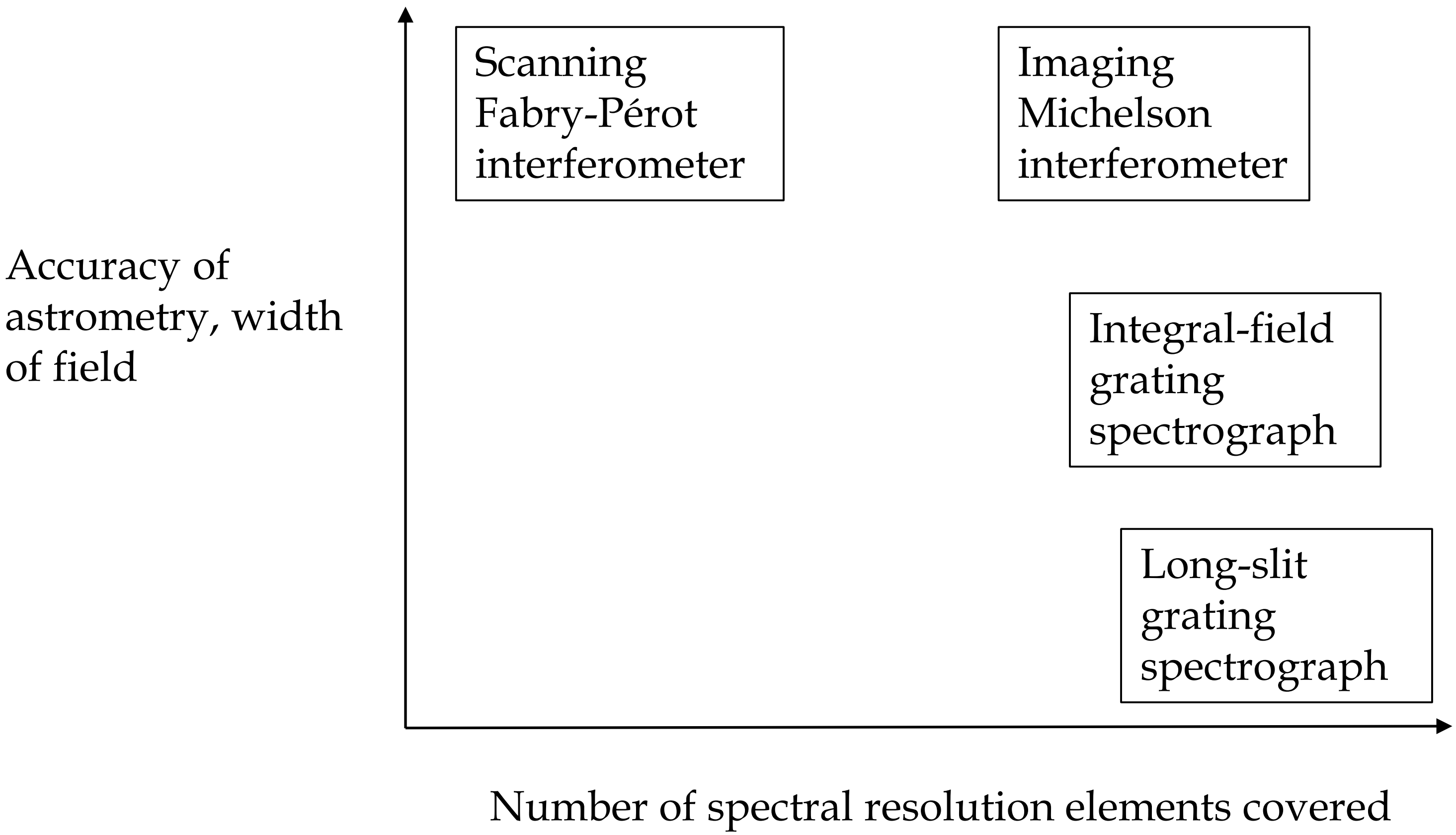

Spectrographs (continued)

Use of detector arrays with such instruments:

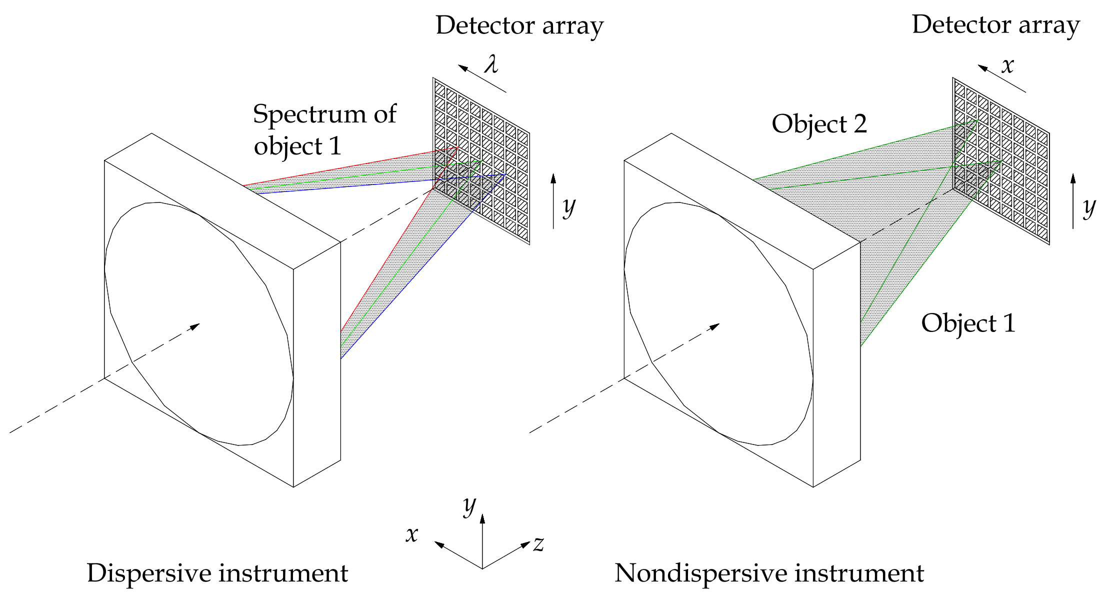

e.g. long-slit grating spectrograph,
integral-field spectrograph

e.g. Fabry-Pérot interferometer,
Michelson interferometer

Scanning Fabry-Pérot interferometer

Best for high-resolution imaging of single lines or line profiles.

- High-reflectivity (r), low-absorption, parallel mirrors whose (wide) optical separation nd can be controlled and scanned precisely.
  - Adjust d: piezoelectric scanning
  - Adjust n: pressure scanning

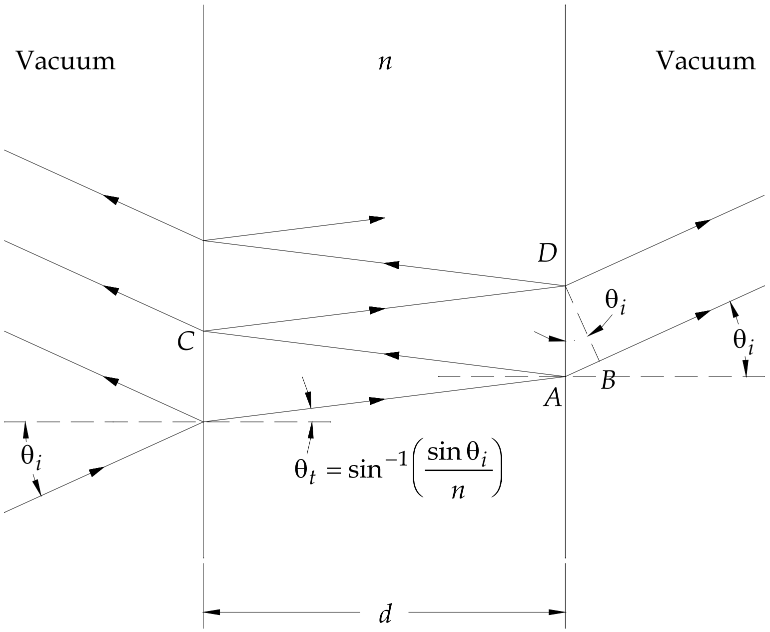

Each pixel sees λ at resolution $\Delta\lambda/\lambda$, where

$$\frac{2\pi dn\cos\theta_t}{\lambda} = \pi m \qquad (m = 0,1,2,\ldots),$$

$$\frac{\Delta\lambda}{\lambda} = \frac{1}{mQ} \quad ,$$

and $Q = \dfrac{\pi r}{1-r^2}$.

Scanning Fabry-Pérot interferometer (continued)

- Usually a sequence of 2-3 FPIs must be used, to isolate a single large-*m* order of the scanning one.

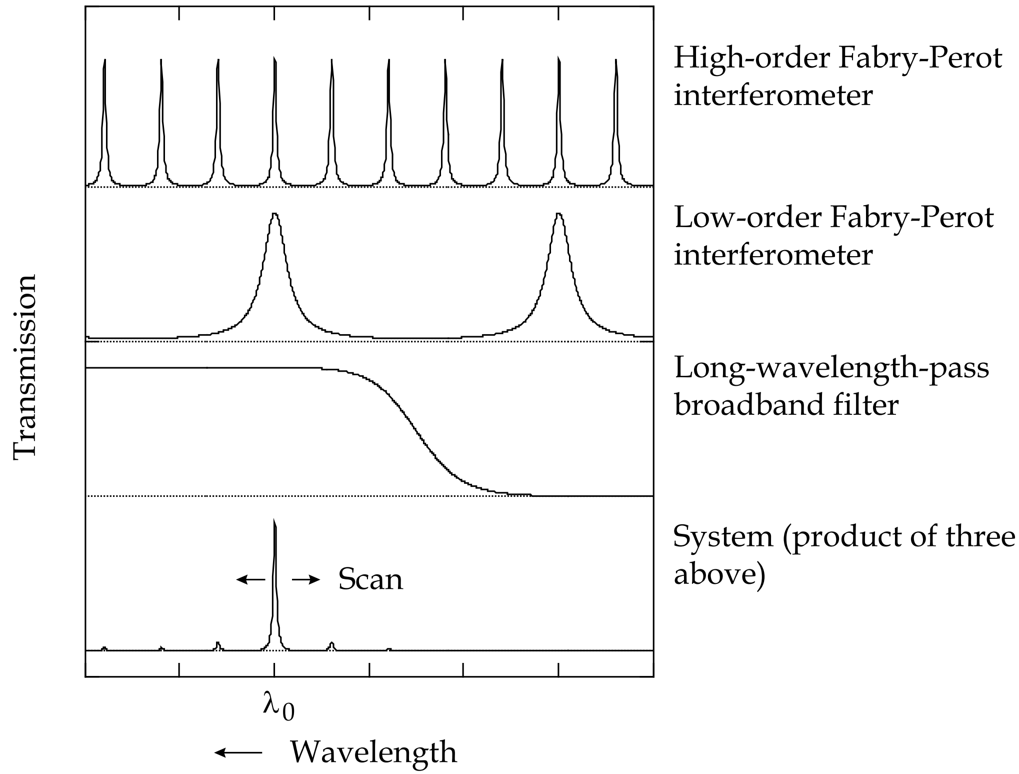

Long-slit grating spectrograph

Best for point sources, or objects in which only one spatial dimension is important.

- ❑ Detector array sees a long wavelength span at pixel along a 1-D strip of the sky.
- ❑ Spectrograph's entrance slit usually 2-10 pixels wide, adjustable for seeing at the cost of spectral resolution.
- ❑ Can only make spectral images by stepping the telescope in the direction perpendicular to the entrance slit, hopefully by a fraction of the slit width per step. (Doesn't work great.)

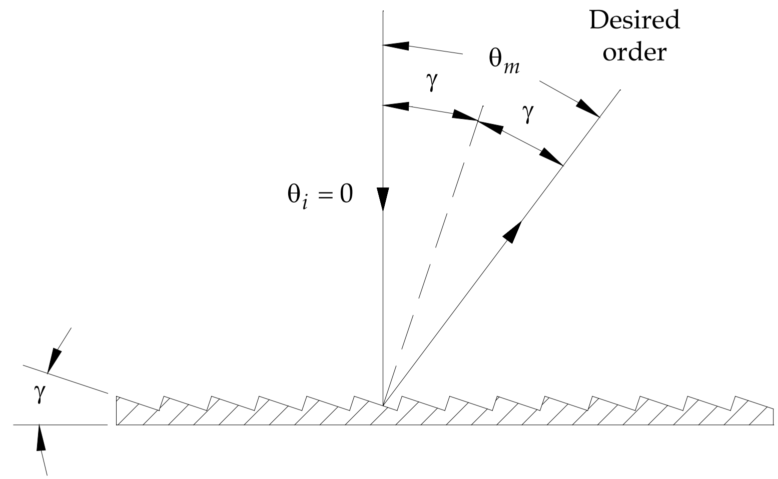

Each pixel sees λ at resolution $\Delta\lambda/\lambda$, where

$a(\sin\theta_m - \sin\theta_i) = m\lambda$, $m = \ldots -2, -1, 0, 1, 2, \ldots$, and

$$\frac{\Delta\lambda}{\lambda} \geq \frac{1}{mN} \quad ,$$

and where N is the number of grating rulings illuminated.

Integral field spectrograph (continued)

Best for full spectra of each pixel in a relatively small neighborhood around a compact object.

- Optically slice up the 2-d field, and image each slice along a different segment of the slit of a grating spectrograph.
- Then reconstruct the data cube after detection.
- Invented by Ira Bowen in the 1930s, before CCDs or computers.

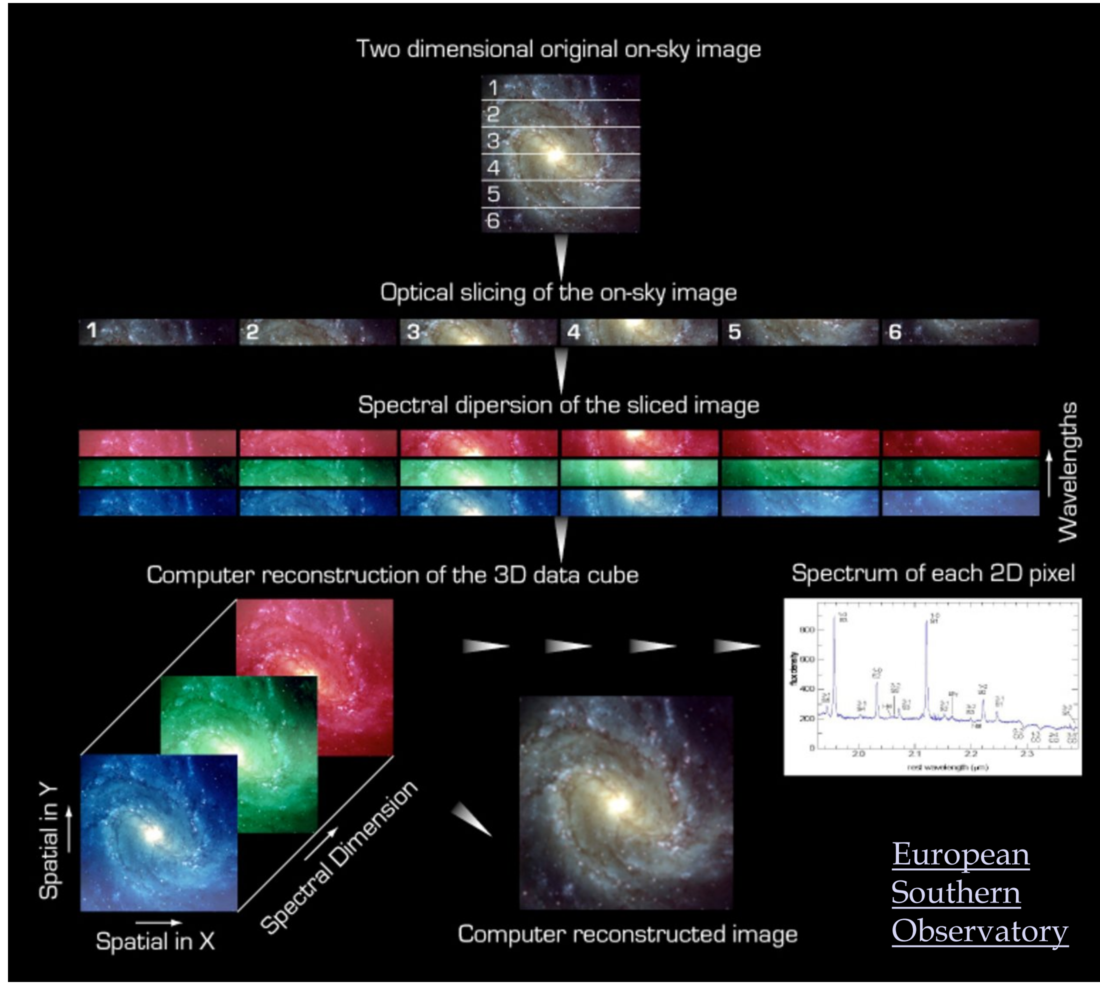

European Southern Observatory

Integral field spectrograph (continued)

- Current implementations feature
  - lenslet arrays, relaying the image to an
  - optical fiber bundle, used to
  - rearrange the image along the spectrograph slit, whence
  - it is detected in long-slit mode, and
  - reconstructed via computer.

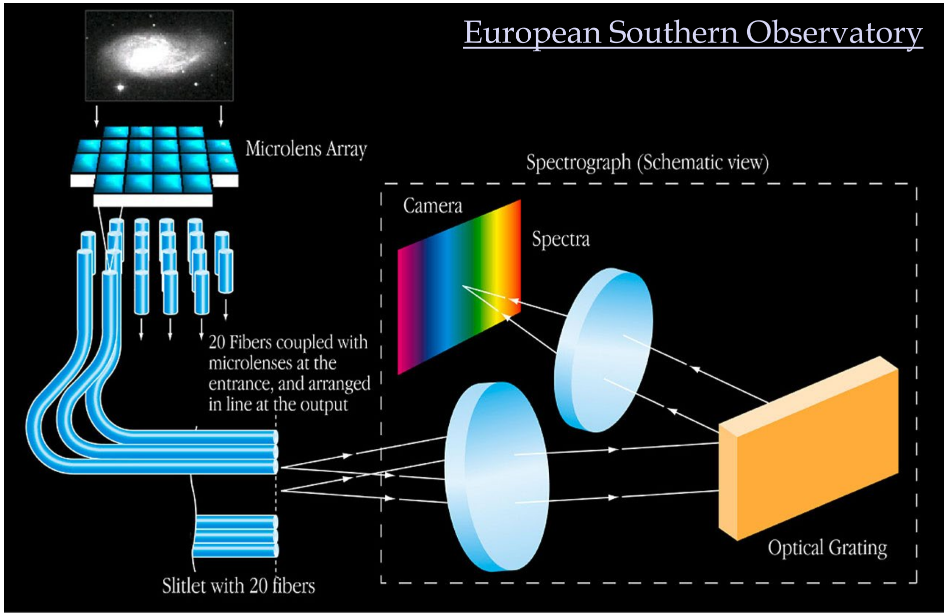

- No light lost at slit due to seeing variation, tracking errors, *etc*. Thus it's great for precision wideband spectra of point sources (i.e. exoplanets).

Imaging Michelson interferometer

Ideally, the best of all: full field imaging, and high-resolution spectra in every pixel.

- Input light is divided with a beamsplitter.
- Half the light is reflected from a stationary mirror…
- the other half from a mirror that can move.
- The light joins up again at the beamsplitter, but half of it has an extra path-length difference from the other half.
- This light is focused on the detector array.

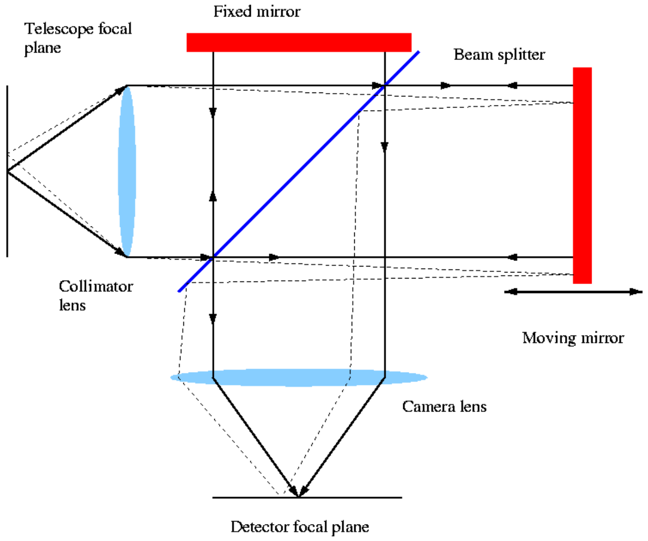

(J. Graham)

Imaging Michelson interferometer (continued)

- The movable mirror is scanned repeatedly over a fixed range.
- Array signal (each pixel) is recorded during the scan, such that the range is sampled finely.
- Average these scan recordings and Fourier-transform the result, and one gets a complete spectrum at every pixel.
    - Wavelength coverage is determined by the sampling rate.
    - Resolution is determined by maximum path-length difference:

$$\frac{\Delta\lambda}{\lambda} = \frac{\lambda}{4d} \quad .$$

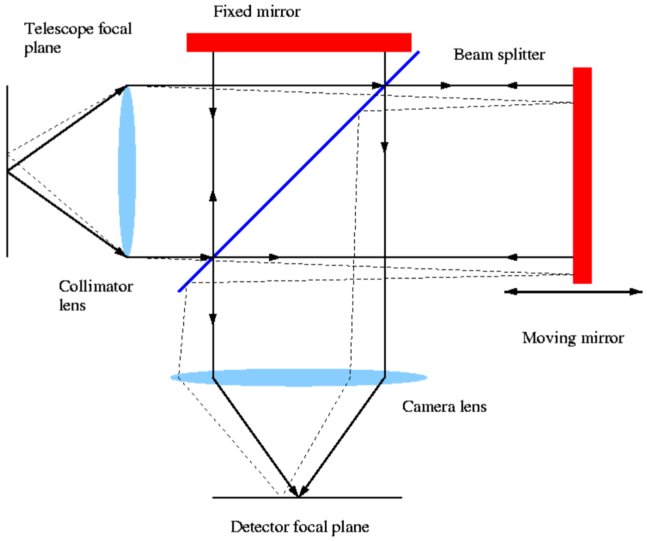

(J. Graham)

Imaging Michelson interferometer (continued)

Down sides:

- Much more complicated than other options; many more challenging high-precision control systems are necessary.
- Thus, expensive.
- Vulnerable to additional sources of noise and systematic error.
- So there aren't many around, yet. One such is SITELLE at the 4-meter Canada-France-Hawaii telescope, which covers the whole visible band (in six chunks) and achieves $\Delta\lambda/\lambda \sim 10^{-4}$ in a 2048×2048 pixel, 11-arcmin square field.

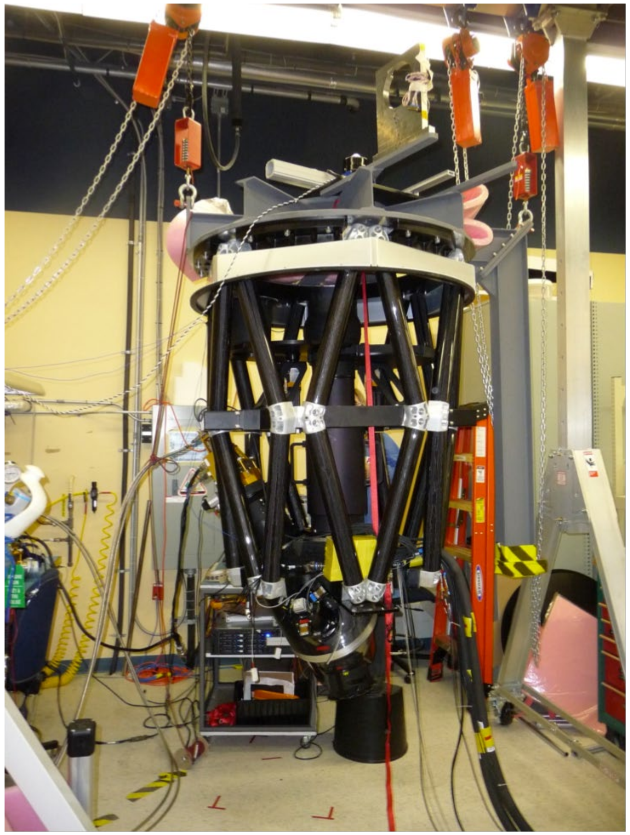

Le Spectromètre Imageur à Transformée de Fourier pour l'Étude en Long et en Large des raies d'Émission.

Spectral lines of atoms and ions at visible wavelengths

In this class we will be concerned with electronic transitions of atoms and ions. They comprise the visible emission from H II regions, planetary nebulae, supernova remnants, and HH objects.

- ❑ Recombination lines of hydrogen (H I)
  - Electric dipole transitions, after recombination in a high-*n* state.
- ❑ Forbidden lines of other elements, like O, O^{+}, O^{++} or S^{+}…
  - …whose forbidden-line spectra are referred to as [O I], [O II], [O III] and [S II], respectively.

Z	Name	Ionization potential (eV)				
		0	+	++	+++	++++
1	**H**	**13.6**				
2	He	24.6	54.4			
3	Li	5.4	75.6	122.5		
4	Be	9.3	18.2	153.9	217.7	
5	B	8.3	25.2	37.9	259.4	340.2
6	C	11.3	24.4	47.9	64.5	392.1
7	N	14.5	29.6	47.4	77.5	97.9
8	**O**	13.6	**35.1**	**54.9**	77.4	113.9
9	F	17.4	35.0	62.7	87.1	114.2
10	Ne	21.6	41.0	63.5	97.1	126.2
11	Na	5.1	47.3	71.6	98.9	138.4
12	Mg	7.6	15.0	80.1	109.3	141.3
13	Al	6.0	18.8	28.4	120.0	153.8
14	Si	8.2	16.3	33.5	45.1	166.8
15	P	10.5	19.8	30.2	51.4	65.0
16	**S**	**10.4**	**23.3**	34.8	47.2	72.6
17	Cl	13.0	23.8	39.6	53.5	67.8
18	Ar	15.8	27.6	40.7	59.8	75.0
19	K	4.3	31.6	45.8	60.9	82.7
20	Ca	6.1	11.9	50.9	67.3	84.5
21	Sc	6.6	12.8	24.8	73.5	91.7
22	Ti	6.8	13.6	27.5	43.3	99.3
23	V	6.7	14.7	29.3	46.7	65.3
24	Cr	6.8	16.5	31.0	49.2	69.5
25	Mn	7.4	15.6	33.7	51.2	72.4
26	Fe	7.9	16.2	30.7	54.8	75.0
27	Co	7.9	17.1	33.5	51.3	79.5
28	Ni	7.6	18.2	35.2	54.9	76.1

The ions on our menu

Lowest-energy states of the ground electronic configurations of O++ and S+, compared to the states of H.

- Note the scale difference between the two plots.
- Only the brightest visible lines are shown.

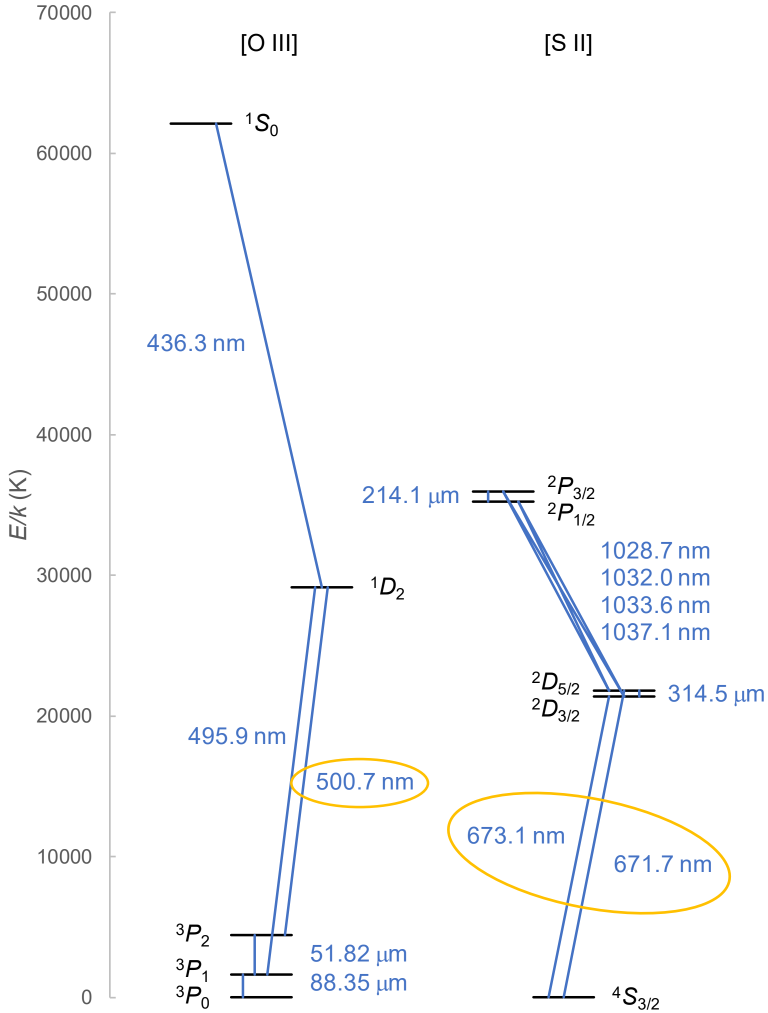

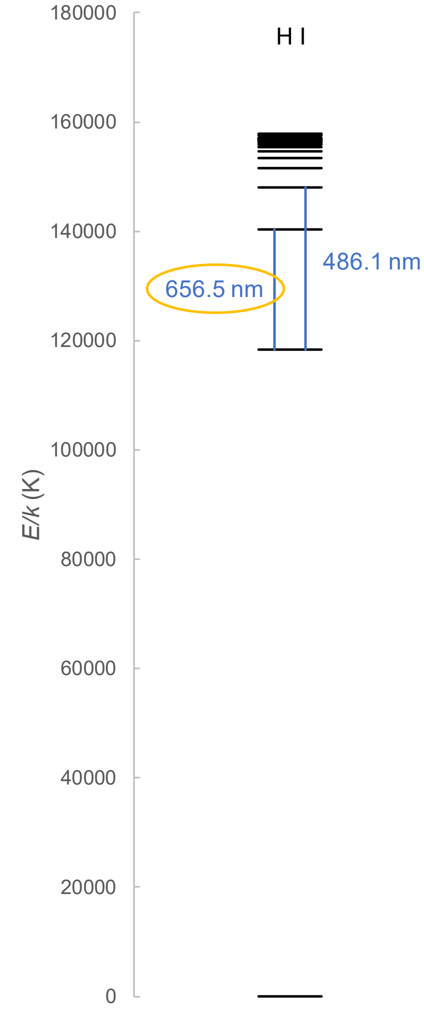

Step 1 of analysis, short form

The main point of the H II region and HH object projects is to make images of the abundance ratios $\chi_{O++} = n(O^{++})/n(H)$ and $\chi_{S+} = n(S^{+})/n(H)$.

- Answers will be very different for the two classes of objects, which you should seek to explain.

- The intensity of an optically-thin *j* to *i* hydrogen recombination line is given, apart from extinction, by

$$I_{ji} = \frac{hc}{4\pi\lambda_{ji}} \alpha_{ji} \int n_e n_p ds \quad ,$$

where I_{ji} is the intensity in erg sec^{-1} cm^{-2} ster^{-1} (which you measure);

λ_{ji} is the wavelength;

$\alpha_{ji}(T)$ is the effective recombination coefficient, in cm^{3} sec^{-1}, calculated quantum-mechanically;

n_e, n_p are number per unit volume of electrons and protons;

and the integral is over distance *s* along the line of sight through the nebula.

Step 1 short form (continued)

- Our recombination line, Hα (j = 3, i = 2), can safely be taken to be optically thin.
- The [O III] and [S II] lines are not recombination lines; they are collisionally excited.
  - Meaning that electrons collide with these ions in their ground state, and leave them in the upper state of the line…
  - whereupon the ion radiates a photon, or collides with another electron, to get back to the ground state.
  - We see the photons that are radiated. The optically-thin intensity of the j to i transition is

$$I_{ji} = \frac{hc}{4\pi\lambda_{ji}} A_{ji} \int n_j ds = \frac{hc}{4\pi\lambda_{ji}} A_{ji} \int f_j \chi n_p ds \quad .$$

- These lines can be taken to be optically thin as well.

Step 1 short form (continued)

- Here

  A_{ji} is the spontaneous radiation rate (Einstein A coefficient) in $\sec^{-1}$;

  n_j is the number density of the ion in state j;

  f_j is the fraction of the ion's population in state j;

  χ is the ratio of the ion's number density to that of hydrogen;

  other terms are as before, and again the integral is over distance s along the line of sight through the nebula.

- We know none of the properties of the nebula *a priori*. Well, almost none: we know that hydrogen densities more than about n_p = 10000 cm^{-3} are very rare outside of neutral molecular clouds.

- This should be compared to the **critical density** of each forbidden line: the density at which the rates of radiative and collisional decay of the upper state are equal.

Step 1 short form (continued)

- If the actual density is much smaller than the critical density, the fraction of the ions in the upper state is given by

$$f_j = \frac{n_e \gamma_{ij}}{A_{ji}} \quad ,$$

where $\gamma_{ij}(T)$ is the collisional excitation rate coefficient in $\mathrm{cm^3\ sec^{-1}}$ of state j. γ_{ij} is also calculated quantum-mechanically.

- This is generally a good approximation for visible forbidden lines. In which case the intensity ratio of a forbidden line and a hydrogen recombination line determines the relative abundance χ: for example, if χ is uniform along the line of sight,

$$I_{\mathrm{H}\alpha} = \frac{hc}{4\pi\lambda_{\mathrm{H}\alpha}} \alpha_{\mathrm{H}\alpha} \int n_e n_p ds \quad , \quad I_{[\mathrm{O\ III}]} = \frac{hc}{4\pi\lambda_{[\mathrm{O\ III}]}} A_{ji} \int \frac{n_e \gamma_{[\mathrm{O\ III}]}}{A_{ji}} \chi_{\mathrm{O}^{++}} n_p ds \quad ;$$

$$\Rightarrow \chi_{\mathrm{O}^{++}} = \frac{\lambda_{[\mathrm{O\ III}]}}{\lambda_{\mathrm{H}\alpha}} \frac{\alpha_{\mathrm{H}\alpha}}{\gamma_{[\mathrm{O\ III}]}} \frac{I_{[\mathrm{O\ III}]}}{I_{\mathrm{H}\alpha}} \quad .$$

The integral cancelled out.

Step 1 short form (continued)

- The only other nuance is that our [S II] filter includes two [S II] lines of similar strength that we can't resolve.

- But this just adds one more term proportional to the S^+ abundance:

$$I_{\mathrm{H}\alpha} = \frac{hc}{4\pi\lambda_{\mathrm{H}\alpha}}\alpha_{\mathrm{H}\alpha}\int n_e n_p ds \quad ,$$

$$I_{[\mathrm{S\ II}]} = \frac{hc}{4\pi\lambda_{[\mathrm{S\ II}]1}}\int n_e \gamma_{[\mathrm{S\ II}]1}\chi_{\mathrm{S}^+} n_p ds + \frac{hc}{4\pi\lambda_{[\mathrm{S\ II}]2}}\int n_e \gamma_{[\mathrm{S\ II}]2}\chi_{\mathrm{S}^+} n_p ds$$

$$= \left(\frac{\gamma_{[\mathrm{S\ II}]1}}{\lambda_{[\mathrm{S\ II}]1}} + \frac{\gamma_{[\mathrm{S\ II}]2}}{\lambda_{[\mathrm{S\ II}]2}}\right)\frac{hc}{4\pi}\chi_{\mathrm{S}^+}\int n_e n_p ds \quad ;$$

$$\chi_{\mathrm{S}^+} = \left(\frac{\gamma_{[\mathrm{S\ II}]1}}{\lambda_{[\mathrm{S\ II}]1}} + \frac{\gamma_{[\mathrm{S\ II}]2}}{\lambda_{[\mathrm{S\ II}]2}}\right)^{-1}\frac{\alpha_{\mathrm{H}\alpha}}{\lambda_{\mathrm{H}\alpha}}\frac{I_{[\mathrm{S\ II}]}}{I_{\mathrm{H}\alpha}} \quad .$$

Step 1 short form (continued)

- The numbers you need are

$$\gamma_{[\mathrm{S\ II}]1} = 6.514\times10^{-9}\ \mathrm{cm}^3\ \mathrm{sec}^{-1} \quad \gamma_{[\mathrm{O\ III}]} = 1.133\times10^{-9}\ \mathrm{cm}^3\ \mathrm{sec}^{-1}$$
$$\gamma_{[\mathrm{S\ II}]2} = 9.702\times10^{-9}\ \mathrm{cm}^3\ \mathrm{sec}^{-1} \quad \alpha_{\mathrm{H}\alpha} = 8.643\times10^{-14}\ \mathrm{cm}^3\ \mathrm{sec}^{-1}$$

- Relative abundance in typical H II regions: $\chi_{\mathrm{O}} = (3.3\pm0.5)\times10^{-4}$, $\chi_{\mathrm{S}} = (1.0\pm0.1)\times10^{-5}$ (McCleod et al. 2016).

- Details: all the recombination coefficients, collision strengths, and A coefficients can be found on line in the CHIANTI atomic database:

  https://www.chiantidatabase.org/chianti.html
  (choose the Direct Access link)

  and references therein.

- The CHIANTI data-file column headers are given by Del Zanna et al. 2015, appendices A1-A2. (Often easier to get the data from the original references.)